Single-Aperture Multiple-Carrier Uplink Using a 20 Kilowatt X-Band Transmitter

T. Cornish[1]

This article describes empirical testing that has been performed on a Deep Space Network 20 kW X-band (7.17 GHz) klystron amplifier. The purpose of these tests is to characterize the intermodulation performance to a level of detail and accuracy not presently provided by theoretical models [1,2]. The data set is sufficiently complete to allow for amplitude and frequency prediction of third-, fifth-, and seventh-order intermodulation products for two or three drive carriers of equal or unequal amplitude. The data can be used for frequency planning and frequency management in a situation where multiple command signals are radiated simultaneously from a single uplink aperture. Although the data have been gathered on a specific make and model of klystron tube (CPI VA876P), it should be extensible to any five-cavity klystron tube since the intermodulation performance is a function of the general tube topology and not subject to unit-to-unit manufacturing variation.

An Excel™ spreadsheet has been assembled to test carrier-frequency combinations for interference. The spreadsheet takes into account uplink signal bandwidth, spacecraft receiver bandwidth, Doppler shift, and acquisition frequency sweeps.

I. Introduction

Future plans for Mars exploration will result in multiple spacecraft in orbit about the planet simultaneously. Several communications strategies are currently under review to allow command of these spacecraft with maximum reliability and performance with minimum cost. One or more of these strategies may require the capability to simultaneously uplink multiple carriers through the same transmitter/antenna subsystem.

Prior attempts to transmit two or more carriers at high power though a single transmitter/antenna subsystem have been hampered by high-order (>100) intermodulation products that interfere with the received downlink [3,4]. Much effort has been expended in the suppression of these high-order intermodulation products with little success [3]. The phenomenon is believed to arise from micro-scale arcing at

[1] Communications Ground Systems Section.

The research described in this publication was carried out by the Jet Propulsion Laboratory, California Institute of Technology, under a contract with the National Aeronautics and Space Administration.

any point illuminated by the uplink that involves a metal-to-metal interface. These include main reflector panels, subreflector panels, subreflector supports, feedcone surfaces, catwalks, gantries, hatches, etc. Welding of such adjacent surfaces seems to have been the only permanent solution so far reported, but this is clearly not feasible for many of the aforementioned structures. Solutions such as aluminum tape have met with partial success, but require frequent, labor-intensive, and ongoing maintenance.

A more cost-effective solution that may fit within Deep Space Network (DSN) future plans would be to use separate apertures for uplink and downlink. This approach would also have the added benefit of reducing the cost and complexity and increasing the performance of the microwave subsystem. Separate paths for uplink and downlink would eliminate the need for diplexers and dichroics, with their associated high cost and impact on received noise temperature.

Having circumvented the problem of high order (>100) intermodulation products by assuming the use of separate transmit and receive apertures, the remainder of the research has concentrated on low-order (<10) intermodulation products. Much empirical evidence exists in the form of nomographs and cardboard slide rules addressing two-tone third-order intermodulation for two carriers of equal amplitude. The author knows of no thorough treatment of products above the third order, with more than two carriers, or with carriers of unequal amplitude. The measurements under these conditions will be important in the prediction of transmitter performance under real-world conditions.

Three tests were conducted: gain and phase versus drive level, two-carrier intermodulation distortion, and three-carrier intermodulation distortion. The test configurations are presented in Section II, and the test results are presented in Section III.

II. Test Configurations

A. Test 1: Gain and Phase Versus Drive Level

The first test that was conducted was a simple power sweep of the klystron amplifier S_{21} magnitude and phase as a function of drive level. The test configuration is shown in Fig. 1. The purpose of this test was to gather data for use by an outside manufacturer to modify an off-the-shelf analog feed-forward linearizer for future evaluation. A Hewlett Packard (HP) 8722 Vector Network Analyzer was used to perform the test. Due to dynamic range limitations of the network analyzer, two sub-tests were performed: one from a reference point of 3 dB gain compression and one from a reference point of 6 dB gain compression.

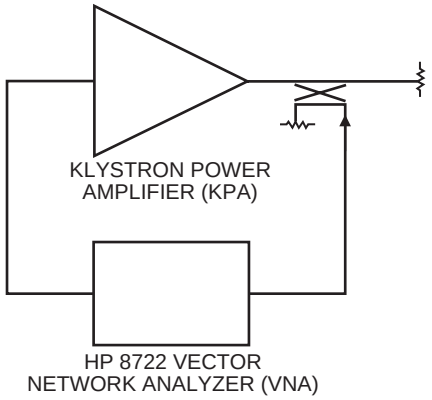

Fig. 1. Test configuration for gain and phase versus drive level.

B. Test 2: Two-Carrier Intermodulation Distortion

The second test that was conducted was a two-carrier intermodulation distortion test. The test configuration is shown in Fig. 2. The klystron amplifier was driven by two synthesizers set to 7165 MHz and 7170 MHz. These frequencies were chosen to be

(1) Centered within the klystron tube instantaneous bandwidth

(2) Spaced far enough apart to be easily resolved on the spectrum analyzer

(3) Close enough together such that all relevant intermodulation products fall well within the klystron tube's instantaneous bandwidth

The output power reference for all of the tests was the point of −6 dB gain compression. Since the absolute output power available varies with the number of carriers and relative carrier level, gain compression serves as a much more repeatable reference than output power.

Measurements were taken first at −6 dB, −5 dB, −4 dB, and −3 dB gain compression. At this point, the measurements were taken at output power back-off levels from the −6 dB compression point, starting at −1.0 dB back off and proceeding in increments of 0.5 dB to −3.0 dB back off, and then in increments of 1.0 dB to −10 dB back off. The rationale for this seemingly complex set of levels is to yield more points where the data are rapidly changing and less points where the slope is nearly constant. The gain compression changes rapidly with drive at high drive levels, offering an accurate and repeatable reference, but very slowly at low drive levels, making the measurement points somewhat ambiguous. Similarly, the output power falls off very slowly with decreasing drive at high drive levels, and can actually increase with decreasing drive between −6 dB and −5 dB gain compression depending on how the particular tube is tuned. At low drive levels, however, the output power drops at nearly the same rate as the drive power, as the klystron tube's operating point moves into the small-signal linear region.

The test was conducted four times—first with equal amplitude carriers, and then with 3 dB, 6 dB, and 10 dB differences in carrier levels. The data were captured by the PC for import and analysis in Excel^{TM}. The test data are presented in Subsection III.B.

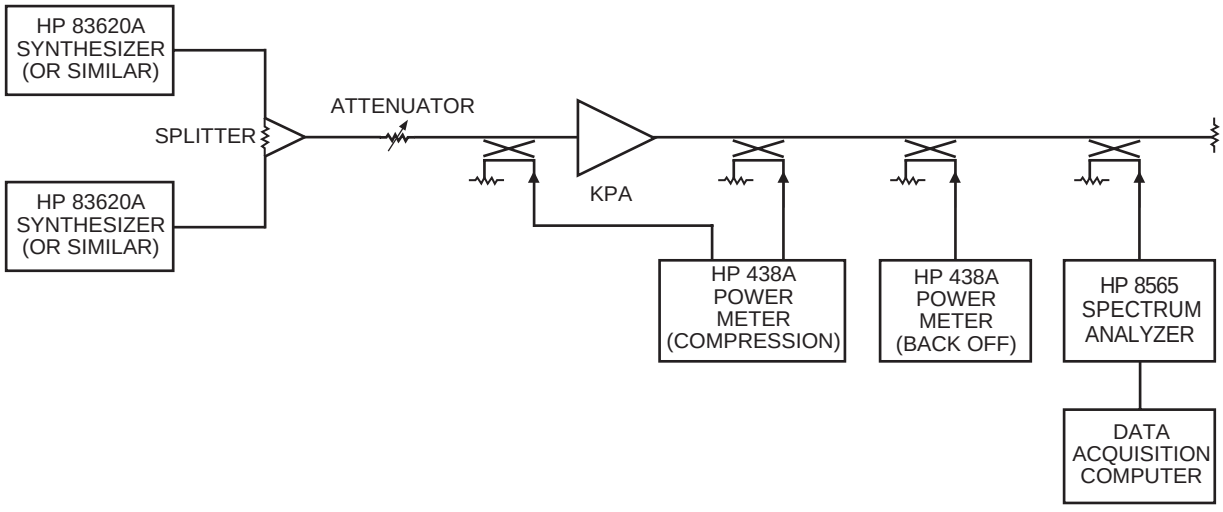

Fig. 2. Test configuration for two-carrier intermodulation distortion.

C. Test 3: Three-Carrier Intermodulation Distortion

The third test that was conducted was a three-carrier intermodulation distortion test. The test configuration is shown in Fig. 3. The klystron amplifier was driven by three synthesizers set to 7165 MHz, 7168 MHz, and 7173 MHz. These frequencies were purposely chosen so that the difference between f_1 and f_2 was not the same as the difference between f_2 and f_3. It was recognized beforehand that if the differences were the same the upper-frequency third-order intermodulation product of f_1 and f_2 would fall squarely on f_3. The lower-frequency third-order intermodulation product of f_2 and f_3 would similarly fall squarely on f_1. The unequal differences allow the individual products to be resolved without any products landing on a carrier or another product.

Measurements were taken at the same power levels as the two-carrier test. The test was conducted seven times—first with equal-amplitude carriers; then with one of the three carriers down 3 dB, 6 dB, and 10 dB; and then with two of the three carriers down 3 dB, 6 dB, and 10 dB. The data were captured by the PC for import and analysis in Excel^{TM}.

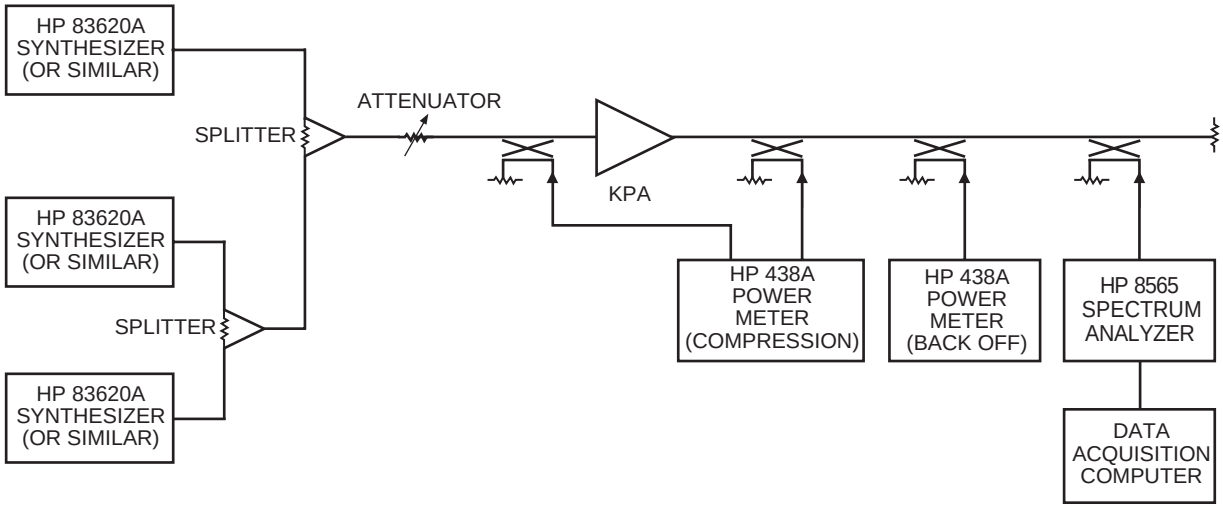

Fig. 3. Test configuration for three-carrier intermodulation distortion.

III. Test Results

A. Test 1: Gain and Phase Versus Drive Level

The results of test 1 are shown in Figs. 4 and 5, respectively. The salient details uncovered by the test are the rates of roll-off of gain and phase. A linearizer would have to be adjusted to have the inverse gain and phase characteristics so that the net transfer function is as linear as possible. The power levels shown on the x-axis are measured at the point that the linearizer would be inserted into the RF drive circuitry in the buffer amplifier assembly.

B. Test 2: Two-Carrier Intermodulation Distortion

The spectrum analyzer was set up as follows:

$$\text{Center frequency} = 7167.5 \text{ MHz}$$

$$\text{Frequency span} = 50 \text{ MHz}$$

$$\text{Resolution bandwidth} = 100 \text{ kHz}$$

$$\text{Vertical bandwidth} = 1 \text{ kHz}$$

$$\text{Sweep time} = 1.3 \text{ s}$$

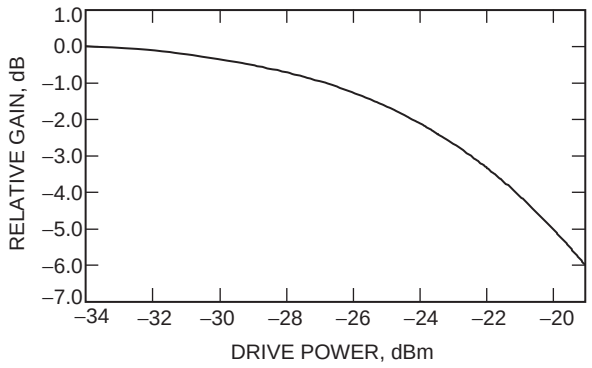

Fig. 4. Magnitude of S_{21} versus drive of the VA876P klystron tube.

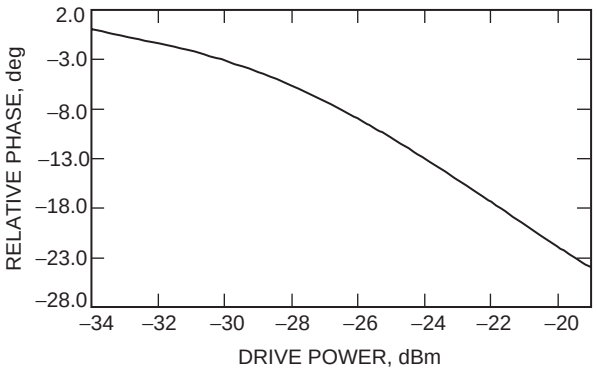

Fig. 5. Phase of S_{21} versus drive of the VA876P klystron tube.

The transmitter was set up as follows:

$$f_1 = \text{ 7165 MHz}$$
$$f_2 = \text{ 7170 MHz}$$
$$\text{Output power} = \text{ 18,500 W at } -6 \text{ dB gain compression}$$

HP VEE™ instrument control software was used to import the spectrum analyzer data into the PC as a text list of values for the 601 sample points. The sample values were then graphed in Excel™ versus frequency. A typical result is shown in Fig. 6. The intermodulation products are at the following frequencies:

$$\text{Third order : } 2f_1 - f_2,\ 2f_2 - f_1$$
$$\text{Fifth order : } 3f_1 - 2f_2,\ 3f_2 - 2f_1$$
$$\text{Seventh order : } 4f_1 - 3f_2,\ 4f_2 - 3f_1$$
$$\text{Ninth order : } 5f_1 - 4f_2,\ 5f_2 - 4f_1$$

A separate worksheet in the workbook was generated for each of the 14 drive levels. A worksheet was then added that scanned the tabular data for the 14 drive levels and found the peak value of each of the intermodulation products. These values were then graphed as a function of output power back off from the point of −6 dB gain compression for the third- through the ninth-order products.

The spectrum analyzer ran out of dynamic range between −50 dBc and −60 dBc, at which point the graph flattens out and the data become useless. This is not seen as a problem, since it is estimated that levels of less than −40 dBc would be well below the noise level by the time they reach the spacecraft. Extrapolation lines were added to the data for two equal carriers to indicate what the data should look like at low drive levels. These lines were not added to the other data sets due to time constraints and the limited value gained by adding them.

At a small signal, the intermodulation products fall off at the following rates:

$$\text{Third order : } 2 \text{ dB/dB}$$
$$\text{Fifth order : } 4 \text{ dB/dB}$$
$$\text{Seventh order : } 8 \text{ dB/dB}$$
$$\text{Ninth order : } 16 \text{ dB/dB}$$

For each combination of carrier levels (equal carriers, 3 dB difference, etc.), two graphs of intermodulation level versus drive were generated. The first graph is the highest of the two products of each order, and the second is the lowest of the two products. For two equal carriers, the levels of the products in each product pair should be the same. Any deviation is measurement variation.

An interesting result is that the products on the side of the lower carrier are lower than the products on the side of the higher carrier by exactly the amount of the difference between the two carriers. This effect is shown in Fig. 7 for a 10 dB difference in the level of the two carriers.

Note that the reference for all of the levels is the highest of the applied carriers. For example, the high-side fifth-order intermodulation product in Fig. 7 is at a level of −38 dBc. The graphs of intermodulation distortion versus output power back off are shown in Figs. 8 through 15. The 0 dB reference on the back-off axis is the point of −6 dB gain compression, corresponding to an output power of between 18,300 W and 18,500 W. The dashed lines in Figs. 8 and 9 indicate theoretical extrapolations below the noise floor of the analyzer.

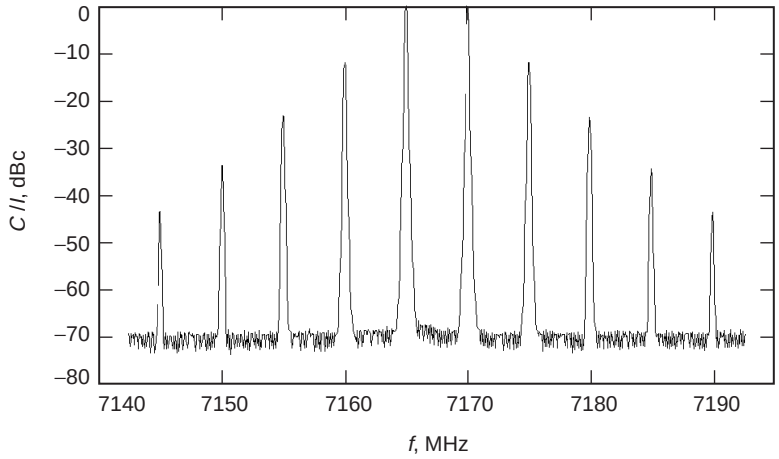

Fig. 6. Intermodulation distortion for two equal carriers at –6 dB gain compression.

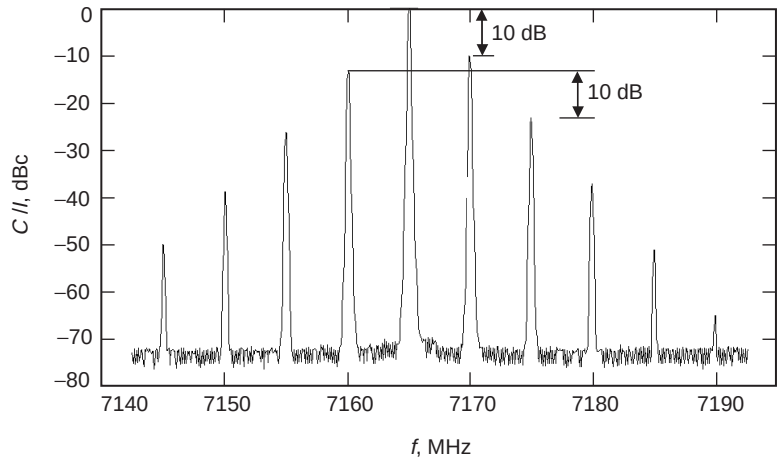

Fig. 7. Two carriers of 10 dB relative amplitude at –6 dB gain compression.

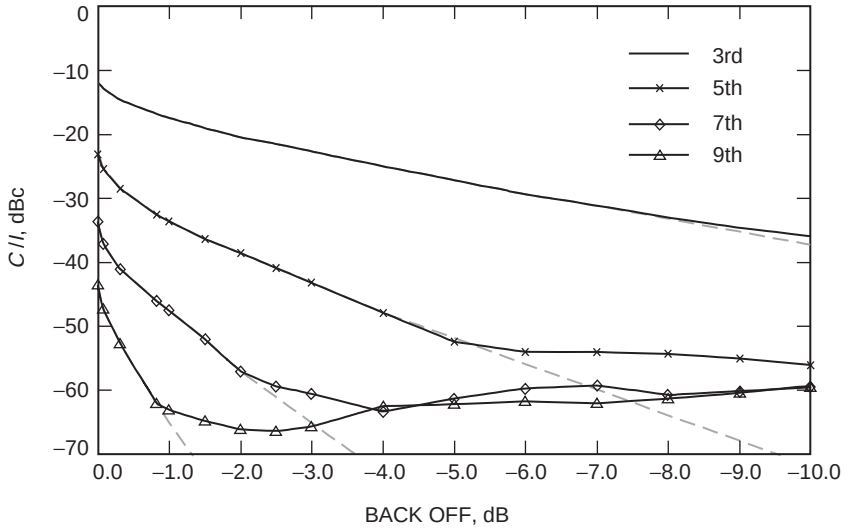

Fig. 8. The highest intermodulation for two equal carriers.

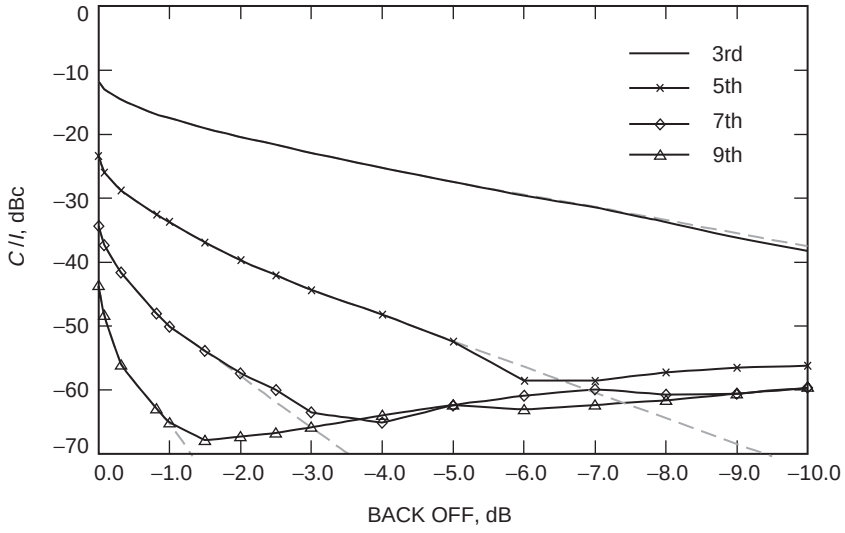

Fig. 9. The lowest intermodulation for two equal carriers.

C. Test 3: Three-Carrier Intermodulation Distortion

The spectrum analyzer was set up as in test 2. The transmitter was set up as follows:

$$f_1 = \text{ 7165 MHz}$$
$$f_2 = \text{ 7168 MHz}$$
$$f_3 = \text{ 7173 MHz}$$
$$\text{Output power} = \text{ 18,500 W at } -6 \text{ dB gain compression}$$

Again HP VEE$^{\text{TM}}$ instrument control software was used to import the spectrum analyzer data into the PC as a text list of values for the 601 sample points. The sample values were then graphed in Excel$^{\text{TM}}$ versus frequency. A typical result is show in Fig. 16. The intermodulation products are at the following frequencies:

$$
\begin{aligned}
\text{Third order}: \quad & f_1+f_2-f_3, f_1+f_3-f_2, f_2+f_3-f_1 \\
& 2f_1-f_3, 2f_1-f_2, 2f_2-f_3, 2f_2-f_1, 2f_3-f_2, 2f_3-f_1 \\
\text{Fifth order}: \quad & 2f_1+f_2-2f_3, 2f_2+f_1-2f_3, 2f_1+f_3-2f_2, 2f_3+f_1-2f_2, 2f_2+f_3-2f_1, 2f_3+f_2-2f_1 \\
& 3f_1-f_2-f_3, 3f_2-f_1-f_3, 3f_3-f_1-f_2 \\
& 3f_1-2f_3, 3f_2-2f_3, 3f_1-2f_2, 3f_2-2f_1, 3f_3-2f_2, 3f_3-2f_1 \\
\text{Seventh order}: \quad & 2f_1+2f_2-3f_3, 2f_1+2f_3-3f_2, 2f_2+2f_3-3f_1 \\
& 3f_1+f_2-3f_3, 3f_2+f_1-3f_3, 3f_1+f_3-3f_2, 3f_3+f_1-3f_2, 3f_2+f_3-3f_1, 3f_3+f_2-3f_1 \\
& 4f_1-f_2-2f_3, 4f_1-f_3-2f_2, 4f_2-f_1-2f_3, 4f_2-f_3-2f_1, 4f_3-f_1-2f_2, 4f_3-f_2-2f_1 \\
& 4f_1-3f_3, 4f_2-3f_3, 4f_1-3f_2, 4f_2-3f_1, 4f_3-3f_2, 4f_3-3f_1
\end{aligned}
$$

Obviously this is more complex than the two-carrier case. This added complexity led to the development of the spreadsheet that will be described in Subsection III. D.

The families of products on each line above share a common set of coefficients and therefore exist at the same amplitude level. For example, the first line of third-order products above has coefficients 1, 1, and −1 in three different permutations. These are the highest three products shown in Fig. 16. The next family has six products with coefficients 2, 0, and −1. These are the next highest six.

Once again, a separate worksheet in the workbook was generated for each of the 14 drive levels, with a fifteenth spreadsheet extracting the peak values of each of the third-, fifth-, and seventh-order intermodulation products. These values were then graphed as a function of output power back off from the point of −6 dB gain compression.

The effect of varying the relative carrier levels is far more complex than in the two-carrier case. As one of the carriers is dropped relative to the other two, the situation degenerates to the two-carrier case, with some of the products dropping sharply and others actually going up. The response of a given product to a change in the amplitude of one of the carriers is a function of the coefficient of that carrier in the definition of the product. For example, the third-order product $2f_1 - f_3$ will be independent of the amplitude of

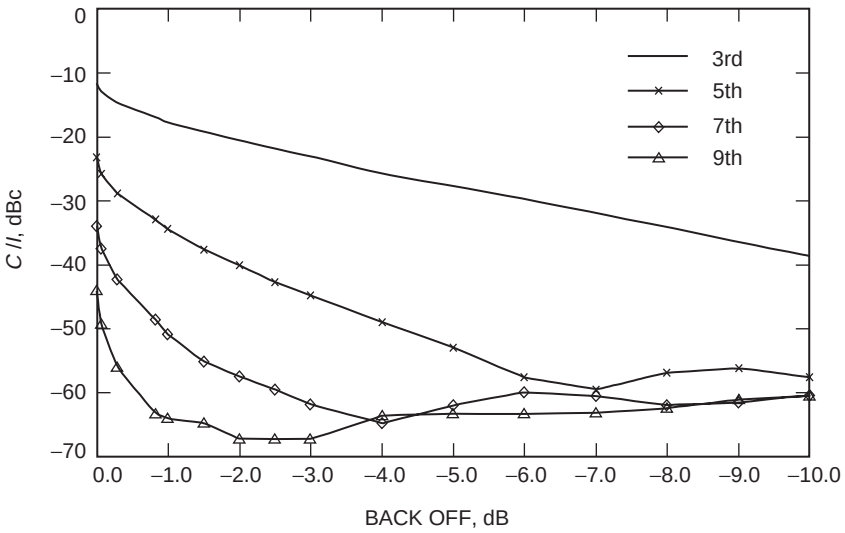

Fig. 10. The highest intermodulation for two carriers 3 dB apart.

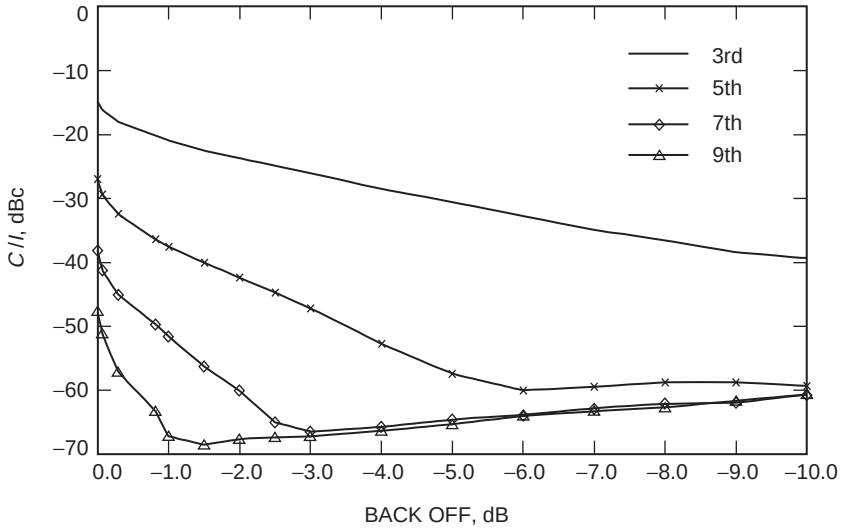

Fig. 11. The lowest intermodulation for two carriers 3 dB apart.

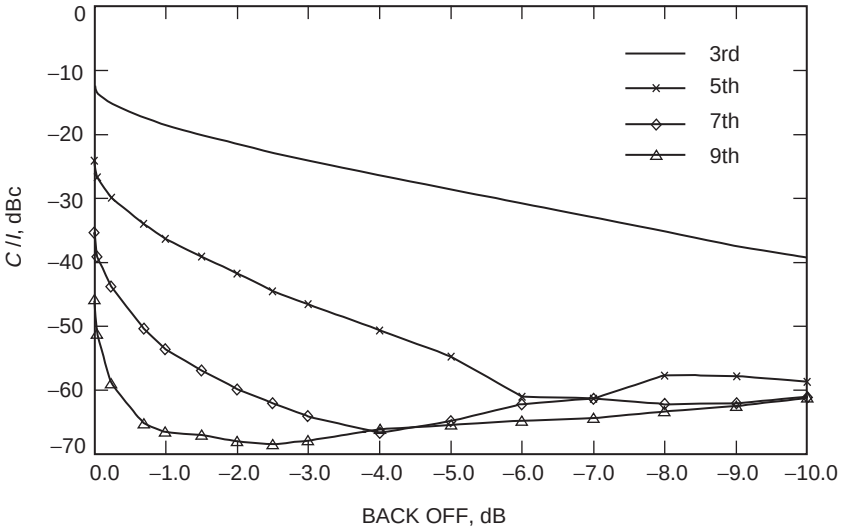

Fig. 12. The highest intermodulation for two carriers 6 dB apart.

f_2, a weak function of f_3, and a strong function of f_1. A suitable general form for the determination of a given product's amplitude given specific carrier amplitudes is yet to be developed. Figure 17 shows the case when one of the carriers is dropped 10 dB relative to the other two. The arrows in Figs. 16 and 17 indicate products that are functions of only f_1 and f_2. It can be seen that they rise as the relative level of f_3 decreases since more power is now made available to these products.

The graphs of intermodulation distortion versus output power back off are shown in Figs. 18 through 24. Only the highest product of each family has been graphed. Note that the reference for all of the levels is the highest of the applied carriers. The notations used in the legends are the coefficients of the carriers in the definitions of the products. The order or the product is the sum of the coefficients. The 0 dB reference on the back-off axis is the point of −6 dB gain compression, corresponding to an output power of between 18,300 W and 18,500 W.

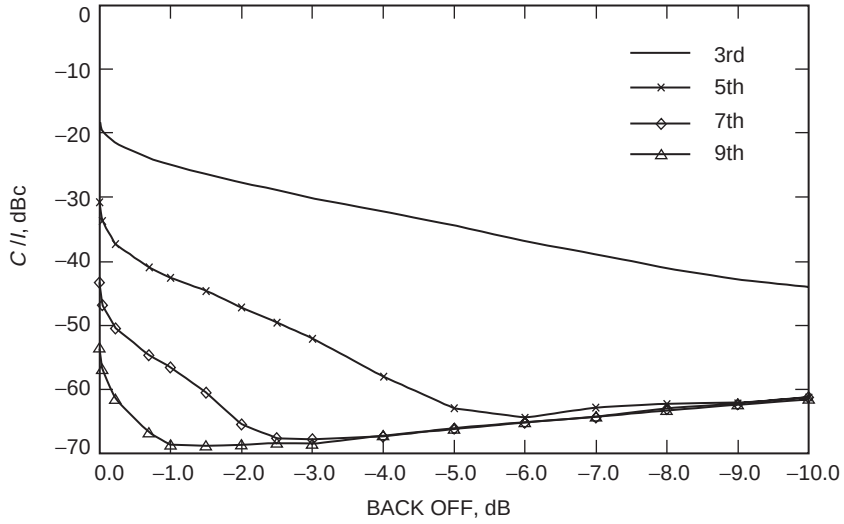

Fig. 13. The lowest intermodulation for two carriers 6 dB apart.

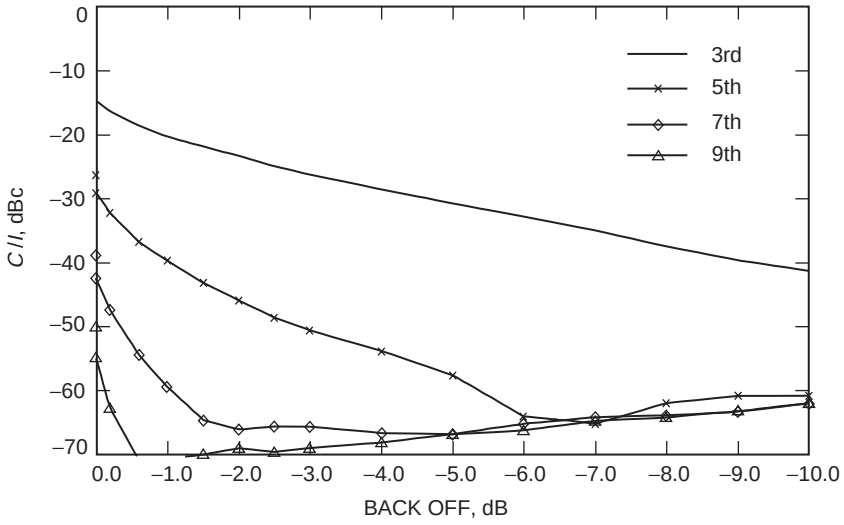

Fig. 14. The highest intermodulation for two carriers 10 dB apart.

D. Spreadsheet for Test of Selected Uplink Frequencies

In the two-carrier case, the selection of uplink frequencies is somewhat trivial. The intermodulation products are spaced above and below the two carriers by the same amount as the frequency spacing between the two carriers. Under the assumption that the two carriers do not interfere with each other, the intermodulation products will not interfere with either of the carriers. One must, of course, take into consideration the bandwidth of the signals and any expected deviation of the center frequency. This deviation would include Doppler shift and any expected sweep range used during spacecraft signal acquisition.

In the three-carrier case, the situation becomes considerably more complicated. If the three carriers are equally spaced, third-order products from one pair of carriers can fall directly on the frequency of the third carrier, resulting in considerable interference and cross talk. Simply choosing unequal frequency spacing does not guarantee that there will be no interference problem. There are 9 third-order products, 15 fifth-order products, and 21 seventh-order products. Add to this the bandwidth of each uplink and the range over which it may be swept and the potential for interference increases dramatically.

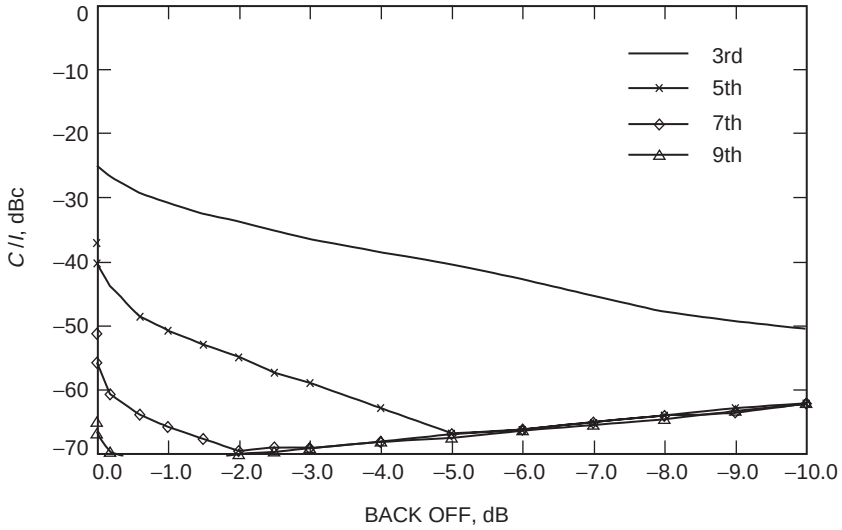

Fig. 15. The lowest intermodulation for two carriers 10 dB apart.

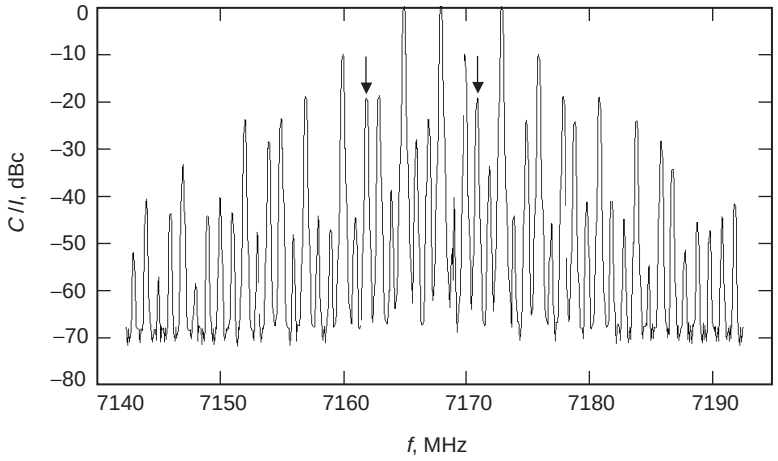

Fig. 16. Intermodulation distortion for three equal carriers at –6 dB gain compression.

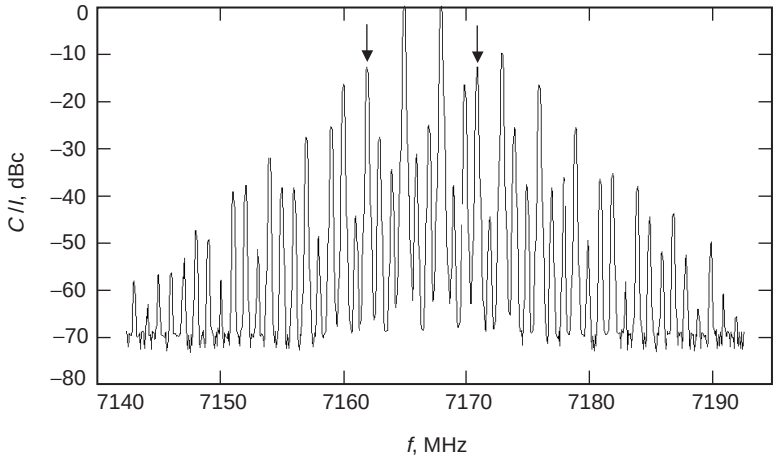

Fig. 17. Three carriers with one at –10 dB relative amplitude.

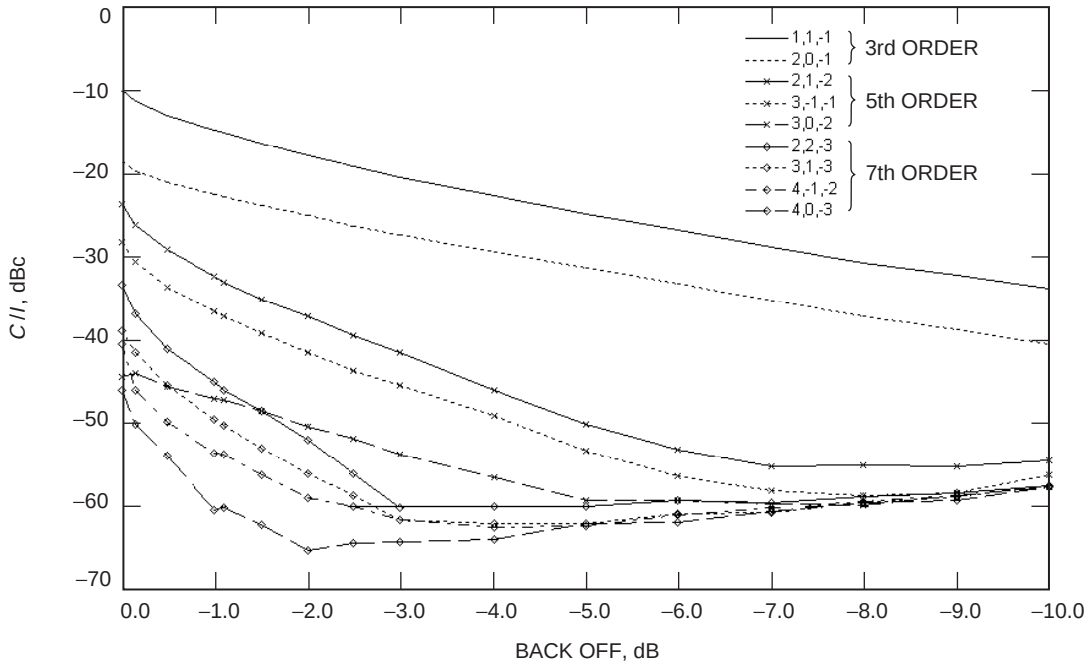

Fig. 18. The highest intermodulation for three equal carriers.

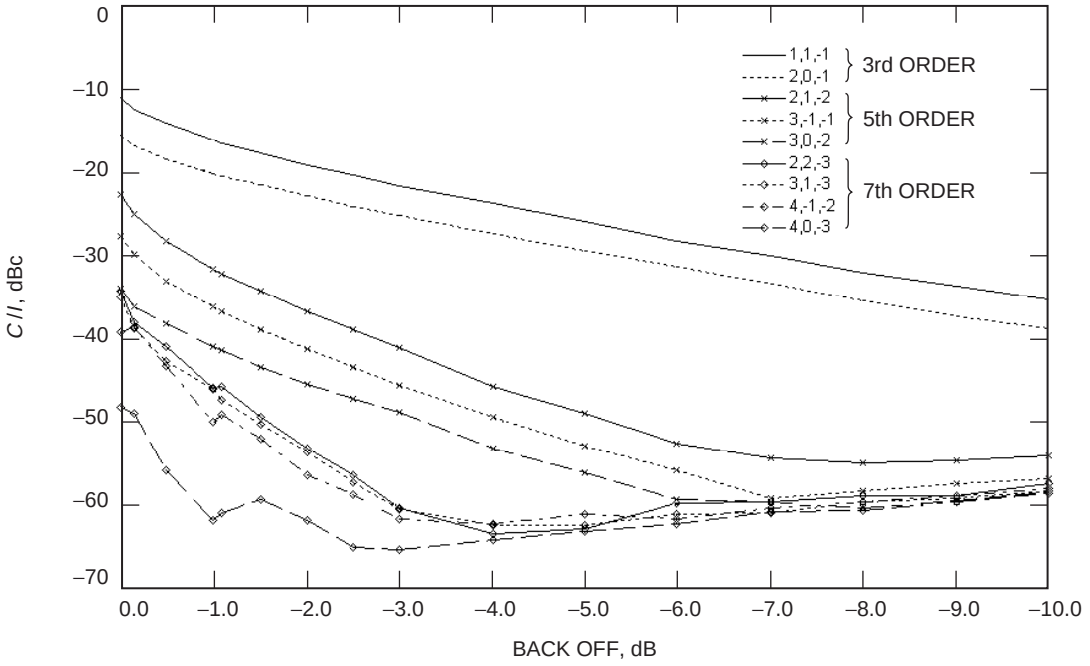

Fig. 19. The highest intermodulation for three carriers with one carrier 3 dB down.

An Excel^{TM} spreadsheet has been devised to assist in the selection of frequencies so as to avoid interference. The spreadsheet takes as input three DNS X-band (7145–7190 MHz) uplink channels, selected from three drop-down lists. For each channel, the user enters an expected peak frequency deviation and desired guard band. The frequency deviation is comprised of one-half of the signal bandwidth plus the expected peak Doppler and acquisition sweep range. The guard band is comprised of one-half of the signal bandwidth plus any safety margin. For instance, a typical command uplink on a 16 kHz subcarrier

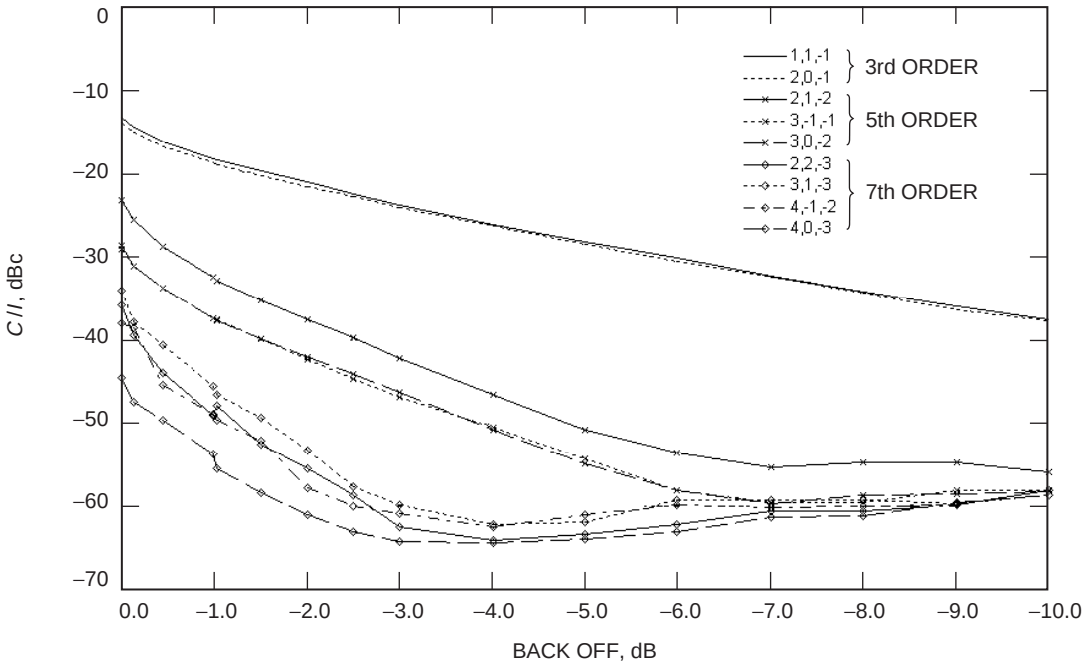

Fig. 20. The highest intermodulation for three carriers with one carrier 6 dB down.

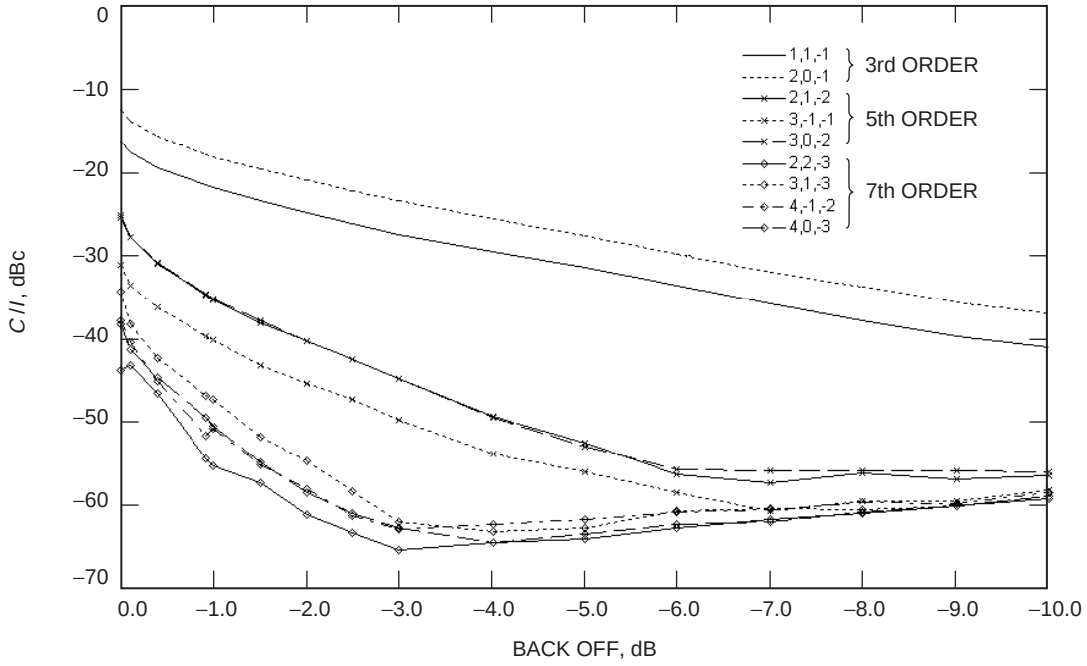

Fig. 21. The highest intermodulation for three carriers with one carrier 10 dB down.

has a 30 dB bandwidth of about 100 kHz (the third sidebands are at ±48 kHz). If the center frequency is expected to be swept ±250 kHz during spacecraft signal acquisition, the peak deviation would be 300 kHz, and the guard band would be a minimum of 50 kHz. The 30 dB bandwidth has been arbitrarily chosen as the point where the signal is low enough not to cause interference and far enough away from the center frequency so as to be outside of the spacecraft receiver bandwidth and, therefore, not subject to being interfered with.

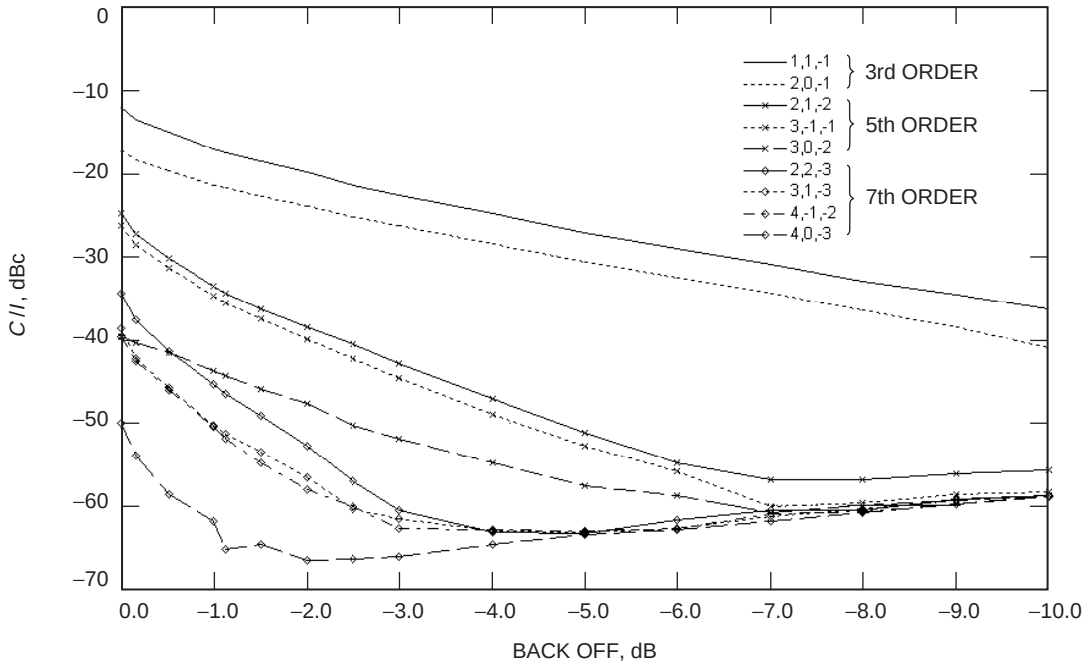

Fig. 22. The highest intermodulation for three carriers with two carriers 3 dB down.

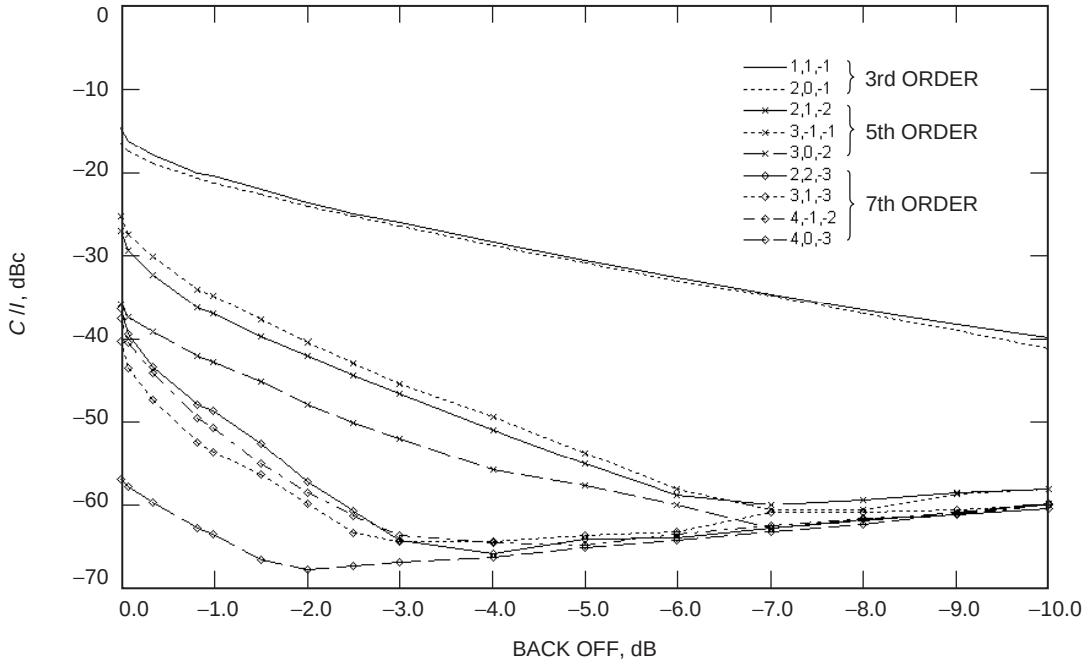

Fig. 23. The highest intermodulation for three carriers with two carriers 6 dB down.

Upon program activation, background VBA (Visual Basic for Applications^{TM}) code steps the three carriers through all possible combinations. The step size for each of the carriers is automatically set to one-half of the guard band. At each step, a check is performed to determine if any of the 45 intermodulation products is within the guard band of any of the three carriers. The spreadsheet dynamically displays the current frequency of each of the carriers, the frequencies of all of the intermodulation products, and the margin between each intermodulation product and each of the three carriers. If an intermodulation

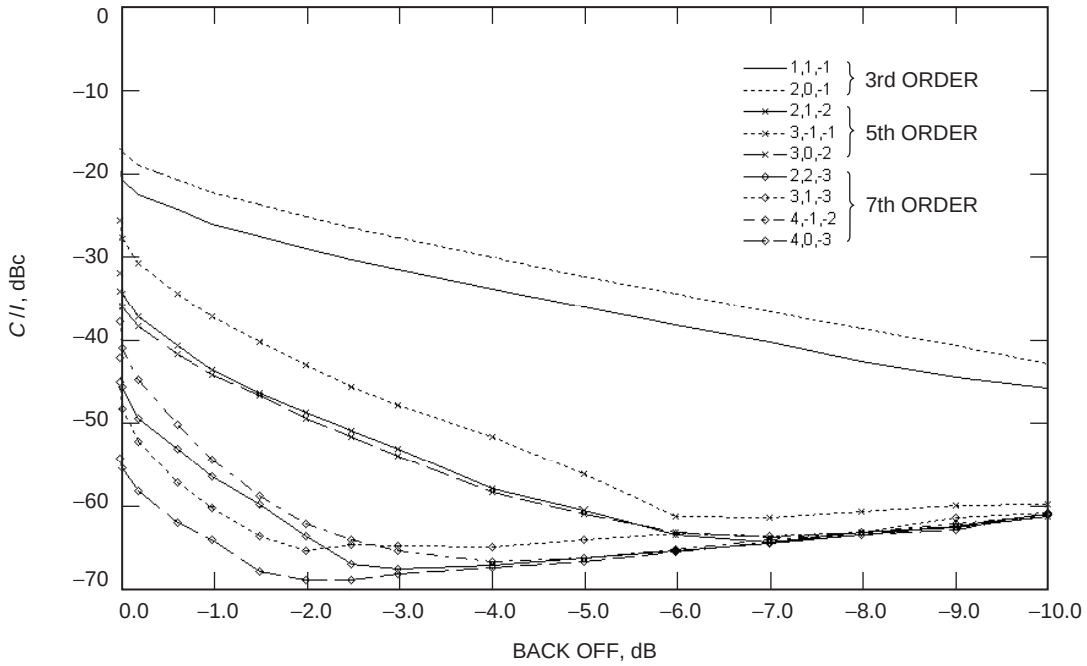

Fig. 24. The highest intermodulation for three carriers with two carriers 10 dB down.

product is found to be within the guard band of any carrier, the program stops and displays an "interference detected" dialogue box. The box gives the user the option of terminating the run or continuing to find any other interference conditions. The specific interference condition is indicated by the spreadsheet cell displaying the margin for that product–carrier combination. The cells are normally the default black on light gray but change to bold white on bright red when the margin drops below the guard band.

At the time of this writing, the program does not give the user any information as to the relative amplitude of an interfering intermodulation product. Cells exist in the spreadsheet for the input of carrier amplitude and the display of intermodulation product amplitude, but these cells have no background code. No suitable mathematical algorithm exists for the calculation of intermodulation product amplitude under anything but the most basic conditions, and time constraints preclude the incorporation of the empirical data into the automated program. The relative amplitude of an interfering product(s) has to be determined by examination of the data as shown in Figs. 8 through 15 for two carriers or Figs. 18 through 24 for three carriers. A sample screen shot of the spreadsheet program is shown in Fig. 25.

IV. Conclusions

A. Receive Band Interference

As discussed in the introduction, micro-scale arcing between adjacent metal-to-metal surfaces illuminated by the beam causes high-order intermodulation products that fall within the receive band. The micro-arcing is a function of peak radiated power and is independent of the number of carriers, but it does not manifest itself as receive band noise in the single-carrier case. The arc constitutes a step nonlinearity in the voltage gradient across the metal-to-metal junction. With one carrier, this step function causes an increase in the broadband noise floor over a wide frequency range centered on the transmit frequency. This increase in the noise floor is difficult to detect because the power is spread evenly over such a broad range that it is on the same order of magnitude as the ambient noise floor.

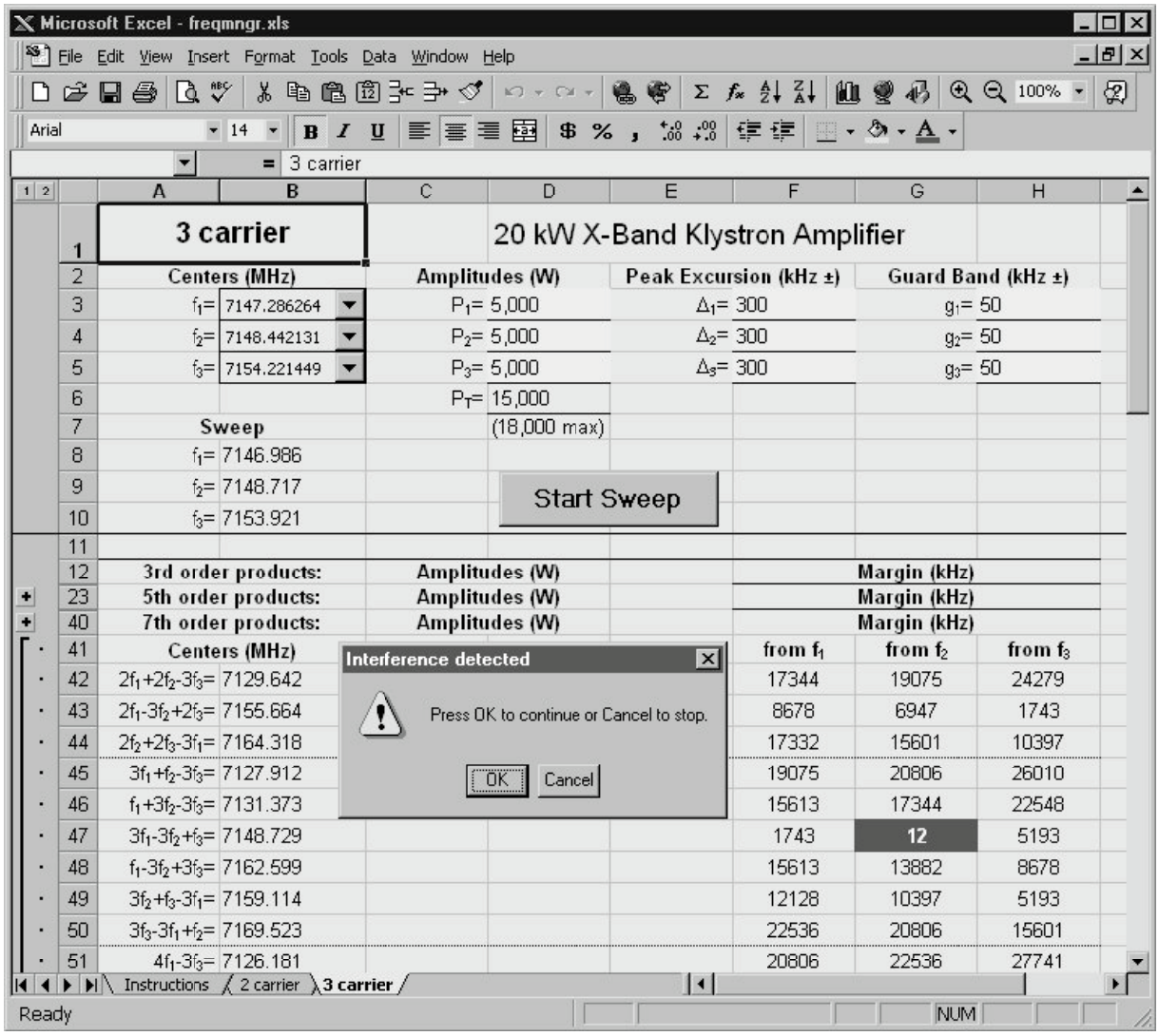

Fig. 25. Frequency selection spreadsheet program.

A smooth nonlinearity such as the klystron-tube saturation characteristic generates intermodulation products that fall off rapidly and are undetectable beyond about the ninth order. A step nonlinearity such as micro-arcing generates intermodulation products that fall off very slowly and are still prominent well beyond the 100th order. Additionally, due to the semi-random nature of the arcing mechanism and the random phasing of several arc sources, the intermodulation products generated are inconsistent in amplitude and spread out in frequency. This effect causes the intermodulation products to take the form of noise bursts rather than discrete spectral lines [4].

Much work has been done in the past to identify and eliminate the various arc sources with little success [3]. The only effective permanent solution has been found to be welding of adjacent surfaces, which clearly is infeasible for many of the antenna structures, such as hatches and hoists. Solutions such as aluminum tape have met with partial success, but require frequent, labor intensive, ongoing maintenance due to weather and wear. Since multiple-carrier uplink is likely to be an occasional rather than a regular operational mode, this ongoing maintenance would be difficult to justify.

Based on these findings, it seems that it would be more cost effective to use separate apertures for transmit and receive during multiple-carrier uplinks. Proposals have been set forth to designate certain antennas, such as the 70-m antennas, as receive only. There has also been discussion on designating separate transmit and receive antennas in beam-waveguide (BWG) clusters, such as DSS 24, DSS 25, and DSS 26. This approach also would have the added benefit of reducing the cost and complexity and increasing the performance of the microwave subsystem. Separate paths for uplink and downlink would eliminate the need for diplexers and dichroics, with their associated high cost and impact on received noise temperature.

B. Two-Carrier Simultaneous Uplink

Under the assumption that the two carriers can be simultaneously transmitted through a linear system without interfering with each other, the nonlinearity of the uplink transmitter does not degrade this capability. The intermodulation products are spaced below the lower frequency carrier and above the higher frequency carrier by the same amount as the frequency difference between the two carriers. Figure 6 illustrates this relationship when the carriers are spaced 5 MHz apart and so are all of the intermodulation products. It is, therefore, impossible for any of the intermodulation products to interfere with either of the carriers unless the carriers themselves overlap. Making sure that they do not overlap must take into account any expected deviation of the center frequency.

Interference with other services outside of the DSN frequency allocation is not believed to pose a problem. Additional harmonics may be generated but will not result in an increase in total harmonic output power. Existing harmonic filtering in the transmitter output will be sufficient to prevent undesirable harmonic radiation.

The klystron tube instantaneous bandwidth is tuned to the same width as the DSN frequency allocation, and the gain falls off rapidly outside the band. At least for the case of the X-band uplink, which is envisioned as the application for this technology, the combination of the klystron passband response and the natural decay of the intermodulation product series for higher orders should ensure that there is no interference with services adjacent to the DSN frequency allocation.

C. Three-Carrier Simultaneous Uplink

The assumption made for two carriers, that the carriers can be simultaneously transmitted through a linear system without interfering with each other, is insufficient to ensure success in the three-carrier case. Even if the three carriers are spaced far apart relative to their respective bandwidths, the possibility for interference exists. If the carriers are spaced apart at equal intervals, the third-order intermodulation product $2f_2 - f_1$ will fall on f_3. Similarly, the third-order intermodulation product $2f_2 - f_3$ will fall on f_1. Choosing unequal spacings for the three carriers is a necessary first step to eliminate this simple problem. Even with unequal carrier spacings, due to the large number of intermodulation products, the potential for interference exists. Adding to this complexity the fact that any or all of the carriers may be sweeping over a nontrivial range exacerbates the task of frequency selection. It has been shown, however, that with careful preplanning it is possible to select three non-interfering frequencies. For example, for three command uplinks on 16 kHz subcarriers that are to be swept ± 250 kHz, DSN X-band uplink channels 1, 2, and 8 are a suitable solution with no interference.

In cases where, due to constraints on frequency selection, three completely non-interfering frequencies cannot be chosen, the data gathered in this study can be used to assess the severity of the interference. For instance, if the interference is caused by a seventh-order product that is 40 dB down, this may not affect the link performance.

V. Recommendations for Further Study

A. Addition of Amplitude Prediction to the Spreadsheet Program

The spreadsheet program currently reports only frequency margins between the intermodulation products and the carriers. Cells have been included for input of the amplitude of each carrier and display of the amplitude of each intermodulation product, but, at the time of this article, these cells are inactive. Since no accurate mathematical model exists for the prediction of the intermodulation product amplitudes, these may have to be determined by indexing into the empirical data gathered in this study.

One possible method of automatically extracting predictions from the acquired data would be to assemble the data into a three-dimensional array with the indices intermodulation order, amplitude delta, and back off. Predictions for a given amplitude delta and back-off value can then be made by interpolation. Separate arrays would be constructed for two-carrier and three-carrier data. The three-carrier case presents a particular problem since the amplitude delta is not a single number. Analysis of the data may uncover some potential simplification, such as considering only the amplitude delta between the highest and lowest carriers, neglecting the middle one. If such a simplification cannot be made, adding another dimension to the array may accommodate the data.

It would be preferable to develop a purely mathematical model that yielded accurate results, at least for products up to the fifth or seventh order. A brief attempt was made to develop such a model by power series analysis similar to that performed by Levitt [1], but using modern hardware and software tools. Gain compression data measured with an HP 8722 Network Analyzer were analyzed in MatLab^{TM}, and a ninth-order power series was generated. The input signal was expressed as the sum of three sinusoidal voltages:

$$A_1 \cos 2\pi f_1 t + A_2 \cos 2\pi f_1 t + A_3 \cos 2\pi f_1 t$$

The input signal expression was evaluated over an array of time values to generate a composite time domain input signal array. This array was then run through the power series polynomial to generate a time domain output array. Finally, a fast Fourier transform (FFT) was done on the output time domain array to generate an output frequency spectrum.

Initial results were aesthetically encouraging, with most of the larger intermodulation products at the correct frequencies and within an order of magnitude of the correct amplitude. It was initially believed that the amplitude of the third-order intermodulation products would be a function of the amplitude of the third-order term of the power series, the fifth-order intermodulation products a function of the fifth-order term, etc. It was felt that the power series coefficients could then be individually manipulated to force the model's prediction to match the measured data.

When this manipulation of power series coefficients was attempted, it became clear that the amplitude of the third-order intermodulation product was very strongly influenced by the amplitude of the fifth-, seventh-, and ninth-order terms of the power series. This effect was mathematically verified as valid and not an artifact of the numerical methods used. Due to time constraints and this added complication, the process did not converge on a useful result. In particular, there is a different delta between groups of intermodulation products of the same order between the model and the measured data. As shown in Subsection III.C, there are two groups of third-order products, three groups of fifth-order products, and four groups of seventh-order products. Manipulation of the power series coefficients was able to force one of the groups to match the measured data, but the other group was incorrect by sometimes over 10 dB. It appears that this discrepancy may be the result of missing or inaccurate higher-order power series terms. A model accurate up to the seventh order may, therefore, require a power series that extends beyond the fifteenth order.

One downfall of the model is that the gain compression data upon which it was based was taken over a relatively small input power range (10 dB). This was sufficient for the linearizer development, but required an extrapolation to develop the mathematical model. The extrapolation necessarily assumed that gain was linear below the lowest measured data point, but this is not really the case. A gain compression measurement over a 30 dB input power range would greatly enhance the accuracy of the first cut at the power series coefficients. With more complete source data, it is conceivable that a model could be developed that is accurate to at least the fifth-order intermodulation product.

It has been suggested that a program might be written to aid in the fine tuning of the power series coefficients. If this could be done successfully, it should be possible to take the concept one step further and eliminate the need for the power function curve fit altogether. Assuming that there exists a power series of some order that yields accurate results, an algorithm could be developed to iterate each of the power series coefficients to reduce the total error between the FFT and the measured spectral data. Once the correct power series coefficients have been determined by matching one set of carrier powers, the model should be able to predict performance with any other combination of carrier powers.

B. Addition of Proactive Frequency Selection to the Spreadsheet Program

Another downfall of the current spreadsheet program is its trial-and-error approach to frequency selection. The user enters a set of DSN uplink channels and waits up to 10 minutes to obtain a result. It would be desirable to configure the program to step through all possible combinations of DSN channels and report a list of suitable channel combinations. To make this practical, it may be necessary to introduce a set of constraints on the choice of channels, such as maximum channel spacing, minimum channel spacing, the use of only the lower one-half of the band, etc. It may take as long as 1 month for a 400 MHz Pentium™ II to test all possible combinations with no constraints. It is not known how large the resultant set of suitable frequencies would be, but it could easily be in the thousands.

C. Spectral Spreading

It has been suggested that the bandwidth of the intermodulation products may be wider than the bandwidth of the original signals. For instance, the first term of the third-order product $2f_1 - f_2$ may be double both the frequency and bandwidth of f_1. Subtracting f_2 would not affect the bandwidth of the composite signal because the modulation of f_1 and the modulation of f_2 are uncorrelated. This effect seems entirely plausible but has not been mathematically or experimentally verified. This issue warrants investigation since it would have to be considered in the formulation of a frequency plan.

D. Performance Verification at a DSN Station

All of the tests performed in this study have been conducted under laboratory conditions on a 20 kW X-band transmitter operating into a water load. The signal sources for all of the tests have been unmodulated carriers. Applicability to actual command uplink signals has been inferred based upon review of the measured output spectrum of a typical Block V exciter. Before the findings of this study are used as a basis for any implementation engineering, it will be necessary to perform tests at an actual DSN station. Performing the measurements should be a simple matter of operating the antenna at zenith and using a spectrum analyzer and simple antenna in the vicinity of the antenna to receive side-lobe energy. All of the measurements are relative, so no calibration of received power would be required.

E. Verification of Linearizer Performance

A feedforward linearizer has been procured for evaluation under this project. This was an additional task that was not in the original project scope. The linearizer should be inserted in the buffer amplifier assembly at the input to the solid-state driver amplifier. The linearizer should improve the intermodulation performance by at least 10 dB at total output power levels of −1.0 dB back off and below.

References

[1] B. Levitt, *Intermodulation Products in Dual Carrier Transmission: Power Series Analysis*, Technical Report 32-1526, vol. XV, Jet Propulsion Laboratory, Pasadena, California, June 15, 1973.

[2] Y. Y. Lau, D. Chernin, C. Wilson, and R. M. Gilgenbach, "Theory of Intermodulation in a Klystron," *IEEE Transactions on Plasma Science*, Special Issue on High Power Microwave Generation, pp. 959–970, June 2000.

[3] D. A. Bathker, D. W. Brown, and S. M. Petty, *Single- and Dual-Carrier Microwave Noise Abatement in The Deep Space Network*, Technical Memorandum 33-733, Jet Propulsion Laboratory, Pasadena, California, August 1, 1975.

[4] B. L. Conroy and D. J. Hoppe, "Noise Bursts and Intermodulation Products Caused by Multiple Carriers at X-Band," *The Telecommunications and Data Acquisition Progress Report 42-127, July–September 1996*, Jet Propulsion Laboratory, Pasadena, California, pp. 1–8, November 15, 1996.
http://tmo.jpl.nasa.gov/tmo/progress_report/42-127/127E.pdf